View metadata, citation and similar papers at core.ac.uk

brought to you by CORE

provided by SJSU ScholarWorks

San Jose State University
SJSU ScholarWorks

Master's Theses

Master's Theses and Graduate Research

1994

Dexterous sliding manipulation using soft fingers

Ying Xue
San Jose State University

Follow this and additional works at: https://scholarworks.sjsu.edu/etd_theses

Recommended Citation
Xue, Ying, "Dexterous sliding manipulation using soft fingers" (1994). *Master's Theses*. 816.
DOI: https://doi.org/10.31979/etd.zdpr-u52c
https://scholarworks.sjsu.edu/etd_theses/816

This Thesis is brought to you for free and open access by the Master's Theses and Graduate Research at SJSU ScholarWorks. It has been accepted for inclusion in Master's Theses by an authorized administrator of SJSU ScholarWorks. For more information, please contact scholarworks@sjsu.edu.

INFORMATION TO USERS

This manuscript has been reproduced from the microfilm master. UMI films the text directly from the original or copy submitted. Thus, some thesis and dissertation copies are in typewriter face, while others may be from any type of computer printer.

The quality of this reproduction is dependent upon the quality of the copy submitted. Broken or indistinct print, colored or poor quality illustrations and photographs, print bleedthrough, substandard margins, and improper alignment can adversely affect reproduction.

In the unlikely event that the author did not send UMI a complete manuscript and there are missing pages, these will be noted. Also, if unauthorized copyright material had to be removed, a note will indicate the deletion.

Oversize materials (e.g., maps, drawings, charts) are reproduced by sectioning the original, beginning at the upper left-hand corner and continuing from left to right in equal sections with small overlaps. Each original is also photographed in one exposure and is included in reduced form at the back of the book.

Photographs included in the original manuscript have been reproduced xerographically in this copy. Higher quality 6" x 9" black and white photographic prints are available for any photographs or illustrations appearing in this copy for an additional charge. Contact UMI directly to order.

U·M·I

University Microfilms International
A Bell & Howell Information Company
300 North Zeeb Road, Ann Arbor, MI 48106-1346 USA
313/761-4700 800/521-0600

Order Number 1358240

Dexterous sliding manipulation using soft fingers

Xue, Ying, M.S.

San Jose State University, 1994

U·M·I
300 N. Zeeb Rd.
Ann Arbor, MI 48106

DEXTROUS SLIDING MANIPULATION USING SOFT FINGERS

A THESIS

PRESENTED TO

THE DEPARTMENT OF MECHNICAL ENGINEERING

SAN JOSE STATE UNIVERSITY

IN PARTIAL FULFILLMENT

OF THE REQUIREMENTS FOR THE DEGREE

MASTER OF SCIENCE

By

Ying Xue

May, 1994

© Copyright 1994 by Ying Xue

All Rights Reserved

APPROVED FOR THE DEPARTMENT OF

MECHNICAL ENGINEERING

Imin Kao (Principal Advisor)

J. C. Wang

William Seto

APPROVED FOR THE UNIVERSITY

ABSTRACT

DEXTROUS SLIDING MANIPULATION USING SOFT FINGERS

by Ying Xue

In this thesis, we build upon the results of the previous sliding manipulation analysis developed for instantaneously dextrous motion analysis, and extend the results to finite motion analysis and trajectory planning for soft robotic fingertips. Using the method of sliding analysis with decomposed rigid-body (RB) and non-rigid-body (NRB) components, we find the trajectory and motions of the fingertips over a finite range of motion during which the RB and NRB components are updated continuously. The results show that, (i) the RB/NRB sliding analysis can be applied to finite motion planning, (ii) the relative magnitudes of RB/NRB motions can be used as an index for manipulation tasks, and (iii) the advantageous orientations of force/motion can be used to plan for the motions of the grasped object. In addition, we discuss how to define the dextrous sliding manipulation in three-dimensional grasping and explore the analytical scheme of solving the 3D problem.

The main contribution of this thesis is the derivation of quasistatic sliding analysis method used to predict the fingertips sliding trajectory that is a basis for general three-dimension trajectory planning with soft robotic fingertips.

Acknowledgements

This work has been supported by the National Science Foundation under Grant IRI-9309823, with additional support from SJSU Foundation.

I would like to express my sincere gratitude to my thesis advisor, Dr. Imin Kao, for all of his guidance and suggestion throughout this research. Special thanks to my thesis readers Dr. J C Wang and Dr. William Seto for their assistance in the completion of this thesis.

Appreciations are also to the National Science Foundation and SJSU Foundation for their support to my research.

Last, but not least, a most special thank you to my wife, Minnie, for all her encouragement, support, and understanding during the time I am writting the thesis.

Contents

1 Introduction **1**

1.1 Introduction 1

1.2 Overview 2

1.3 Literature Review 3

1.4 Nomenclature 5

2 2D Dextrous Sliding Manipulation **7**

2.1 Theoretical Background 7

2.2 Properties of the Friction Limit Surface (FLS) 8

2.3 Equations of Quasistatic Sliding Analysis 9

2.3.1 Static Force and Moment Equilibrium 11

2.3.2 Kinematics for Dextrous Manipulation 12

2.4 Solving for the Motion of Fingertips and Card 13

3 3D Trajectory Planning for Multi-finger Grasp **17**

3.1 Problem Statement 17

3.2 Friction Limit Surface in 3D Space 19

3.3 Force and Moment Equilibrium 20

3.4 Kinematics of Dexterous Sliding Motion 24

4 Simulation Results and Discussion **26**

4.1 Overview 26

4.2 2D Simulation Results and Discussion 27

4.3 3D Simulation Results and Discussion 29

5 Conclusion and Future Work **34**

5.1 Conclusions 34

5.2 Future Work 35

Appendices **36**

A Derivation of Equations in Chapter 2 **36**

A.1 Jacobians of Two Fingertips 36

A.2 The Weighting Matrices 37

A.3 RB/NRB Components of the Fingertips 37

B Derivation of Equations in Chapter 3 **39**

B.1 Solving the Sliding Angle β 39

B.2 Geometry Parameters 40

B.3 The expression of External Moment M_b 40

C Simulation Programs **41**

C.1 Manipulating a Card with Two Sliding Soft Fingertips 41

C.2 Manipulating a Hemi-ellipsoid Using Three Soft Fingers 47

List of Figures

2.1 Friction limit surface for a soft finger 8

2.2 A business card under sliding manipulation with two soft fingertips . 10

2.3 This figure shows force and moment equilibrium at a position after the grasped object has been rotated for an angle of q from its original position. The local coordinates (x and y) at the contact also change their orientations by angle q. 12

2.4 A figure shows the velocities of the fingertip with respect to the local coordinates, xy. y' is the coordinate of the contact when the orientation is at q_0 angle. ω is the instantaneous angular velocity of the card when the contact is at point P. 13

2.5 Trajectory of the fingertip for the sliding manipulation task with respect to the fixed XY coordinates. Note that when the two fingers are aligned with each other at the end of the sliding manipulation, the card ceases to move since there is no RB motion. 15

3.1 Hemi-ellipsoid grasped by three soft robotic fingertips 18

3.2 Friction limit surface in force/moment three-dimensional space 19

3.3 Grasp and friction force at contact points 21

3.4 Velocities of the fingertips at contact 23

4.1 Angular velocity of the card, ω, vs. the independent parameter, τ. As τ increases, ω decreases and approaches zero asymptotically. 28

4.2 Velocities of fingertips showing the RB and NRB components for the sliding manipulation. The manipulation starts with large effective RB components and ends with only NRB components when the card stops moving. 29

4.3 Rotational velocity of the object with respect to the object coordinate system $P(XYZ)$ 32

4.4 Fingertip sliding angle with respect to the local coordinate system $P_i(l_i m_i n_i)$ 33

Chapter 1

Introduction

1.1 Introduction

Manipulating an object with soft fingers will cause sliding and rolling at contacts, *i.e.*, *dextrous manipulation*. We consider the grasped fingers as soft fingers since not only the grasped forces, but also the friction moments at the centroid of the contact are transmitted.

Trajectory planning for dextrous manipulation is one of the important applications in robotic research. In this thesis, we study the problem of dextrous manipulation with soft robotic fingers. Analysis in 2D field is based upon the previous dextrous sliding motion analysis [Kao and Cutkosky 1992, Kao and Cutkosky 1993], where a model for instantaneous quasistatic sliding manipulation is proposed and simulation results are presented.

To illustrate the procedure of solving the trajectory planning problem in three dimensions, a hemi-ellipsoid model grasped by three soft robotic fingertips will be studied. Dextrous sliding motion exists at the contacts between the surface of grasped object and fingertips. The normal contact forces (f_{ni}) and the absolute velocities of the fingertips (v_i) will be controlled. First, we will derive the friction forces and moments of fingertips by using friction limit surface and force/moment equilibrium equation, *i.e.*, the basic requirements to achieve a quasistatic sliding motion. Second, the quasistatic sliding analysis will be implemented to find the trajectories of the fingertips and the motion of the object.

1.2 Overview

Chapter 2 is an extended study of two-dimensional field analysis proposed by [Kao and Cutkosky 1992]. We will review the theoretical background of quasistatic sliding analysis, i.e., some properties about the soft fingers and discuss the kinematics of dextrous sliding manipulation and the solution of finite motion planning with sliding fingers. Finally, a manipulation task involving two soft fingers will be discussed with simulation results. The relationships between the relative magnitude of RB and NRB components and the motion of the grasped object during the manipulation will also be investigated.

Chapter 3 will explore the analytical scheme and solution of 3D dextrous sliding manipulation. A hemi-ellipsoid model grasped by three soft robotic fingertips will be

presented to illustrate the whole procedure of solving the trajectory planning problem. The simulation result shows that dextrous sliding analysis is a reliable method to predict the trajectories of fingertips and the motion of object.

Chapter 4 will present the simulation results in 2D and 3D examples. In addition, we will discuss the effects of RB/NRB motion as an index for dextrous manipulation and the effects of friction moment on the rotation of the object.

Finally, conclusions and future work will be discussed in Chapter 5.

1.3 Literature Review

Related motion planning analysis has been studied in the areas such as: planning for dextrous manipulation with sliding and rolling contacts [Trinkle 1989, Rus 1992, Kao and Cutkosky 1992, Kao and Cutkosky 1993, Chong *et al.* 1993, Sarkar *et al.* 1993]; compliant motion of dextrous hands and control [Mason and Salisbury 1985, Michelman and Allen 1993]; and the problems of predicting the motion of the grasped object [Mason 1985, Peshkin and Sanderson 1988b, Peshkin and Sanderson 1988a]; contact mechanics and limit surfaces [Goyal *et al.* 1991, Montana 1988].

In 1992, Kao and Cutkosky proposed a method for modeling dextrous manipulation with sliding fingers and described, (i) how the motion of a grasped object and fingers according to external force and moment; (ii) how to control the fingertips so that the fingers and grasped object will follow a desired trajectory. Late in 1993,

theoretical analysis for dextrous manipulation with sliding was compared with the experimental results [Kao and Cutkosky 1993].

1.4 Nomenclature

P_i	Contact centroid between ith fingertip and the surface of object.
$O(XYZ)$	Object coordinate system.
COR	Center of rotation of the card.
$P_i(l_i m_i n_i), P_i(XY)$	Local and object coordinates system attached at ith contact P_i.
f_i	Force applied by ith fingertip at contact P_i.
f_{ni}	Normal grasp force of fingertip at ith contact P_i.
f_{ti}	Friction force between fingertip and object at ith contact.
f_{li}, f_{mi}	Components of friction force f_{ti} in l and m axes, respectively.
F_b, M_b	External force and moment applied on the object.
m_{ni}	Friction moment applied by fingertip in n axis at contacts.
$\mathbf{P}$	An unit vector normal to the friction limit surface.
r_i	A vector giving the position of ith contact P_i with respect to the center point B.
α	An angle between axes m_i and Z.
β	An angle between fingertip velocity v_i and x_i axis in 2D field. An angle between friction force f_{ti} and l_i axis in 3D field.
μ	Coulomb coefficient of friction.
λ	Ratio of the maximum moment and maximum friction force.
v_i	Absolute velocity of ith fingertip.
v_b	Absolute velocity of the grasped object.

v_s	Relative sliding velocity of the fingertip with respect to the object.
v_{sl}, v_{sm}	Components of sliding velocity in l and m axes.
v_{rb}, v_{nrb}	Rigid body and non rigid body velocity of the fingertip.
$v_{rb,slip}, v_{nrb,slip}$	Rigid body and non rigid body sliding velocity of the fingertips.
$\mathbf{W}$	Concatenated weighting matrix.

Chapter 2

2D Dextrous Sliding Manipulation

2.1 Theoretical Background

In the scope of this chapter, we assume that the geometry of the rigid object and the stiffness of the fingertips are known. As we know from the previous research, when the velocity and acceleration of the sliding fingertips are sufficiently small, the relative motion between a grasped object and the sliding fingertips can be treated as quasistatic motion. At each instantaneous position, we can apply the static force and moment equations to the grasped object. Also, the force and motion of the fingertips have to satisfy the contact kinematics, such as the limit surface for soft fingers with finite contact areas and Coulomb friction model for hard fingers with negligible contact areas.

In this thesis, we will concentrate on the finite motion planning of the robotic

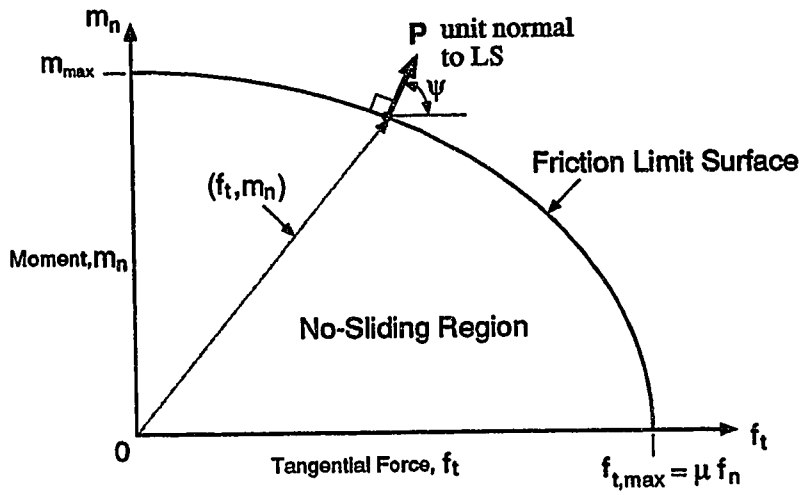

Figure 2.1: Friction limit surface for a soft finger

manipulator with soft-finger contacts. A case study for a two-fingered manipulation task will be presented.

2.2 Properties of the Friction Limit Surface (FLS)

The motion of soft fingers can be described by the friction limit surface [Goyal *et al.* 1991, Kao and Cutkosky 1992] and static equilibrium equation for the quasistatic analysis. 2D friction limit surface is approximated by an elliptical curve as shown in Figure 2.1. Before setting up these equations, we first introduce some properties of the friction limit surface that are used specifically in the analysis of sliding manipulation.

1. The friction limit surface is approximated by the elliptical curves, called *limit surface*, as shown in Figure 2.1. It can be obtained, by simulation or experiments,for any soft contact if we know the contact shape, pressure distribution,

and the coefficient of friction [Goyal *et al.* 1991, Lee 1991].

2. When the tangential force and moment are located inside the friction limit surface, *i.e.*, the *no-sliding region*, there is no relative motion between fingertips and object. The soft fingertips and the object will move together as an integrated unit. As we increase the tangential force and moment to the friction limit surface, sliding starts between the fingertips and the object. We can apply the sliding analysis to find the motion of the fingertips as well as the object [Kao and Cutkosky 1992]. As we increase force/moment to regions outside the limit surface, acceleration of motions at contact will occur.

3. The direction of the fingertip sliding velocity (both translational and rotational) must be parallel to the unit normal vector $\mathbf{p}$ of the limit surface at the force and moment (f_t, m_n), as shown in Figure 2.1.

2.3 Equations of Quasistatic Sliding Analysis

Kao and Cutkosky [1992] proposed a model in analyzing and solving the motions of dextrous manipulation with sliding fingertips. The theoretical prediction of the instantaneous planned trajectory was later verified by experimental results [Kao and Cutkosky 1993].

Figure 2.2 shows the example of a business card that is supported by a smooth table surface. Two soft fingers contact at axisymmetric positions with same force,

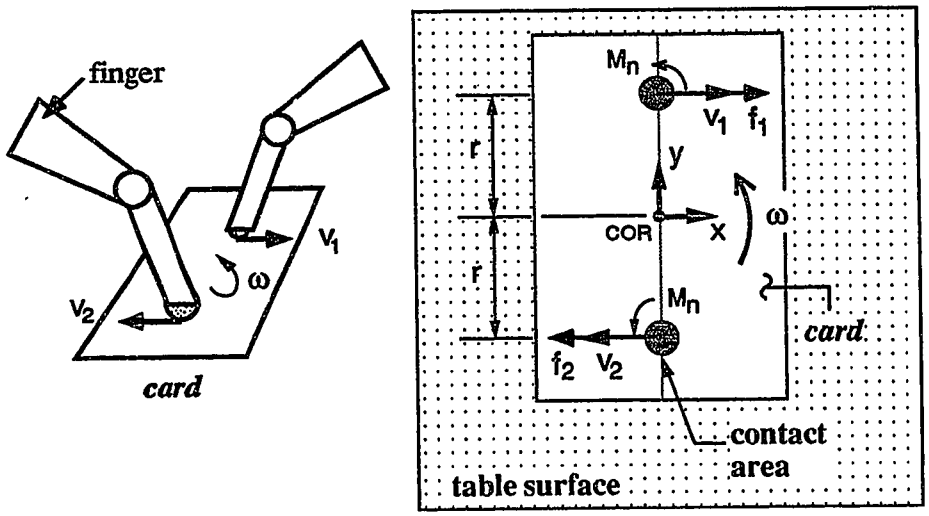

Figure 2.2: A business card under sliding manipulation with two soft fingertips

moment, and velocity to manipulate the card with sliding. We ignore the dry friction force between the table top and the card since it is relatively small compared to the friction force between the soft fingertips and the card surface. When we start move the fingertips, the fingertips not only rotate together with the card (rigid-body motion) but also slide on the contact areas (non-rigid-body motion). In this manipulation task, we maintain the fingertips' tangential forces along the X-direction with a force control scheme. Our purpose is to find the trajectories of the fingertips, the history of the angular velocity of the card, rigid-body and non-rigid-body motions of the fingertips, and the relative magnitude of the RB and NRB components as an index to the motion of the grasped object.

2.3.1 Static Force and Moment Equilibrium

In terms of the friction limit surface shown in Figure 2.1, the equation of elliptical curve can relate the tangential force and moment of fingertips by

$$f_t^2 + \frac{m_n^2}{\lambda^2} = (\mu \cdot f_n)^2 \tag{2.1}$$

where $\lambda = \frac{m_{n,max}}{\mu \cdot f_n}$ is a constant for any given soft contact with known normal force, μ is the friction coefficient. For this two-dimension quasistatic sliding, we can apply equations of equilibrium on the two constraints at the contact (the tangential force f_t and normal moment m_n). Figure 2.3 shows the force and moment of fingertips applied on the card, where XY is the fixed reference frame, xy is the moving frame oriented with the grasped object at the contact, and q is the reference angle of rotation with respect to the XY frame. The new equation of equilibrium is

$$f_t \cdot r \cdot \cos(q) = m_n \tag{2.2}$$

Solving equations (2.1) and (2.2) for f_t and m_n, we find,

$$\begin{cases} f_t = \frac{\lambda \cdot \mu \cdot f_n}{\sqrt{\lambda^2 + r^2 \cdot \cos^2(q)}} \\ m_n = f_t \cdot r \cdot \cos(q) \end{cases} \tag{2.3}$$

When the card rotates from $q = 0°$ to $90°$, the magnitudes of tangential force and moment are varying according to the friction limit surface, changing the ratio of m_n/f_t from the largest value to minimal values and finally to zero (see Figure 2.1).

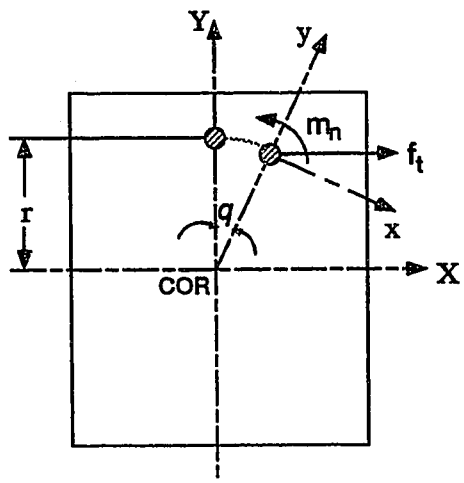

Figure 2.3: This figure shows force and moment equilibrium at a position after the grasped object has been rotated for an angle of q from its original position. The local coordinates (x and y) at the contact also change their orientations by angle q.

2.3.2 Kinematics for Dextrous Manipulation

According to the friction limit surface and the plasticity theory, the direction of motion at the sliding contacts is $\mathbf{p}$, which is related to f_t and m_n by the equation of the ellipse. Hence, the equation $\frac{dr/d\tau}{d\theta_n/d\tau} = \frac{v_{slip}}{\omega} = \lambda \cdot \cot\psi$ relates the relative magnitude of the linear component $dr/d\tau$ to the rotational component $d\theta_n/d\tau$ [Kao and Cutkosky 1992], where τ is an independent parameter such as the arc length of the motion trajectory. Therefore, we can write

$$\begin{cases} v_{slip} = c \cdot \lambda \cos\psi \\ \omega = c \cdot \sin\psi \end{cases} \tag{2.4}$$

where c is a scaling constant with unit of rad/sec.

Figure 2.4 shows the coordinates and motion of fingertips after the object (card) has been rotated for an angle of q from its initial orientation. In Figure 2.4, $B(XY)$

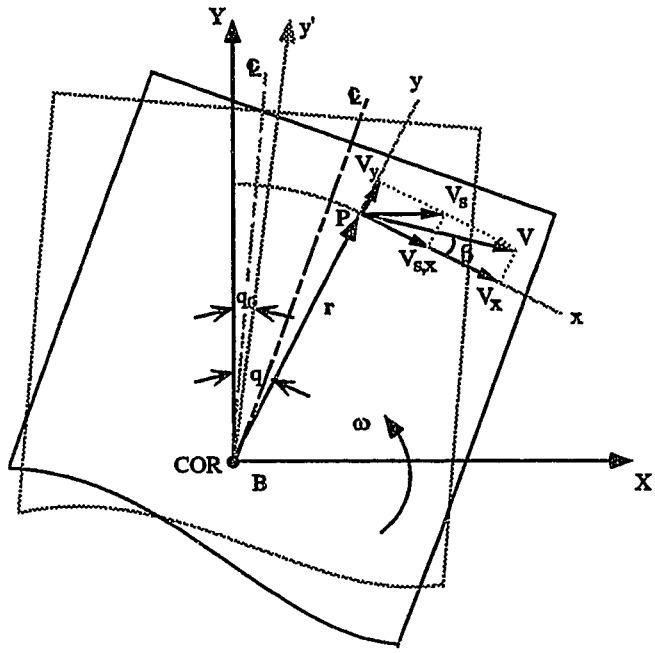

Figure 2.4: A figure shows the velocities of the fingertip with respect to the local coordinates, xy. y' is the coordinate of the contact when the orientation is at q_0 angle. ω is the instantaneous angular velocity of the card when the contact is at point P.

and $P(xy)$ are the coordinate systems fixed at the center of rotation (COR) and the centroid of the contact at P, respectively. The distance "r" is the length between points B and P, which is called the characteristic length of the grasp.

2.4 Solving for the Motion of Fingertips and Card

The problem we are addressing is: "What would be the trajectory of the grasped object and RB/NRB components of fingers if the forces and moments applied at fingertips are specified for sliding manipulation?"

We need two sets of equations to solve the problem. One is the velocity compatibility equation and the other is the minimization criteria of NRB motions that was developed by Kao and Cutkosky [1992]. The velocity compatibility equation is given by the equation: ${}^{P}_{B}\mathbf{J}\mathbf{v}_b = \mathbf{v} + \mathbf{v}_{slip}$, whose elements can be broken into RB and NRB components except $\mathbf{v}_b$, that is,

$$ {}^{P}_{B}\mathbf{J} \cdot \mathbf{v}_b = \underbrace{\mathbf{v}_{rb} + \mathbf{v}_{nrb}}_{\mathbf{v}} + \underbrace{\mathbf{v}_{rb,slip} + \mathbf{v}_{nrb,slip}}_{\mathbf{v}_{slip}} . \tag{2.5} $$

where ${}^{P}_{B}\mathbf{J}$ is the coordinate transformation matrix. An objective function, "g", defined as the weighted norm of the NRB vector is

$$ g = \frac{1}{2} \cdot \mathbf{v}_{nrb}^{T} \cdot \mathbf{W} \cdot \mathbf{v}_{nrb} \tag{2.6} $$

where $\mathbf{W}$ is the weighting matrix for the fingertip involved in manipulation (details are given in the Appendix A. We select the weighted norm of the NRB motions as the objective function so that the NRB motions are minimized with respect to the grasp orientation. The weighting matrix, $\mathbf{W}$, not only provides dimensional homogeneity for the norm of $\mathbf{v}_{nrb}$ but also scales the linear and angular components of $\mathbf{v}_{nrb}$ according the grasping configuration. In addition, we define v_h as the RB part of the the fingertip velocities with respect to $B(XY)$. We then express the relative rigid-body motion of the object with respect to the fingertips as $v_b' = v_b - v_h$ [Kao and Cutkosky 1992].

We can apply the above equations to solve for v_b' by minimizing the g function. By concatenating equations for the two fingers, we obtain

$$ (\mathcal{J} \cdot \mathbf{v}_b' - \mathbf{v}_{slip})^{T} \cdot \mathcal{W} \cdot \mathcal{J} = 0, \tag{2.7} $$

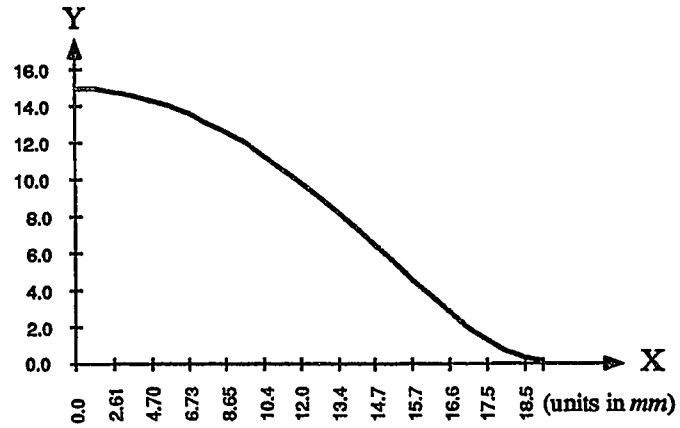

Figure 2.5: Trajectory of the fingertip for the sliding manipulation task with respect to the fixed XY coordinates. Note that when the two fingers are aligned with each other at the end of the sliding manipulation, the card ceases to move since there is no RB motion.

where, $\mathcal{J} = \begin{bmatrix} {}^{P}_{B}\mathbf{J}_1 & 0 \\ 0 & {}^{P}_{B}\mathbf{J}_2 \end{bmatrix}$, and $\mathcal{W} = \begin{bmatrix} \mathbf{W}_1 & 0 \\ 0 & \mathbf{W}_2 \end{bmatrix}$. The resulting $\mathbf{v}_b'$ can be found.

$$v_b' = \begin{bmatrix} 0 \\ 0 \\ \frac{1}{2r} \cdot c(\sin\psi - \lambda\cos\psi\cos(q)) \end{bmatrix} \tag{2.8}$$

With v_b' in equation (2.8), we can determine the RB and NRB components of the fingertips (see Appendix 1). Therefore, the angular velocity of the card is

$$\omega = -\frac{v \cdot \cos(\beta)}{r + \lambda \cdot \cot\psi \cdot \cos(q)} \tag{2.9}$$

where the negative sign indicates a clockwise rotation. Note that when $q = 0°$, equation (2.9) reduces to the instantaneous results as presented by [Kao and Cutkosky 1993]. The angle β is the angle between the velocity of the fingertip, $\mathbf{v}$, and the local

x coordinate, as shown in Figure 2.4. The angle β can be expressed as

$$tan(\beta) = \frac{\lambda \cdot \cot\psi \cdot \sin(q)}{r + \lambda \cdot \cot\psi \cdot \cos(q)} \tag{2.10}$$

In this case study, we maintain a force control scheme along the X direction; therefore, the relative sliding velocity is always parallel to the X-direction. The trajectory of the fingertip is obtained from the orientation of the card and the sliding motion of the fingertips with respect to the card. For the purpose of implementing the sliding simulation, the position of the contact centroid with respect to the fixed reference coordinate system $B(XY)$ is

$$\begin{cases} X = r \cdot \sin(q + \delta q) - v_{slip} \cdot \delta\tau \\ Y = r \cdot \cos(q + \delta q) \end{cases} \tag{2.11}$$

where, $\delta q = \omega \cdot \delta\tau$ is the angle of increment during simulation, and τ is an independent parameter used in simulation. After each step increment, we need to update the length r and rotation angle q according to

$$\begin{cases} r = \sqrt{X^2 + Y^2} \\ q = \frac{\pi}{2} - \arctan\frac{Y}{X} \end{cases} \tag{2.12}$$

Afterwards, we have to update all the values from equations (2.3) to (2.4) and (A.1) to (A.2) for the next orientation. The simulation results will be discussed in Chapter 4.

Chapter 3

3D Trajectory Planning for Multi-finger Grasp

3.1 Problem Statement

Most research in sliding analysis has been concerned with multifinger in 2D space. However, our fingertips often grasp and manipulate a 3D object. Thus, the sliding analysis has to be extended to 3D field. During grasped manipulating, fingertips slide and roll on the surface of the object which are the main factors affecting the motion of the fingers and grasped object. In the scope of the thesis, however, we only consider the sliding motion and also make the following assumptions.

1. The soft contact area is homogenerous so that we can only consider the moment normal to the tangential plane at contacts.

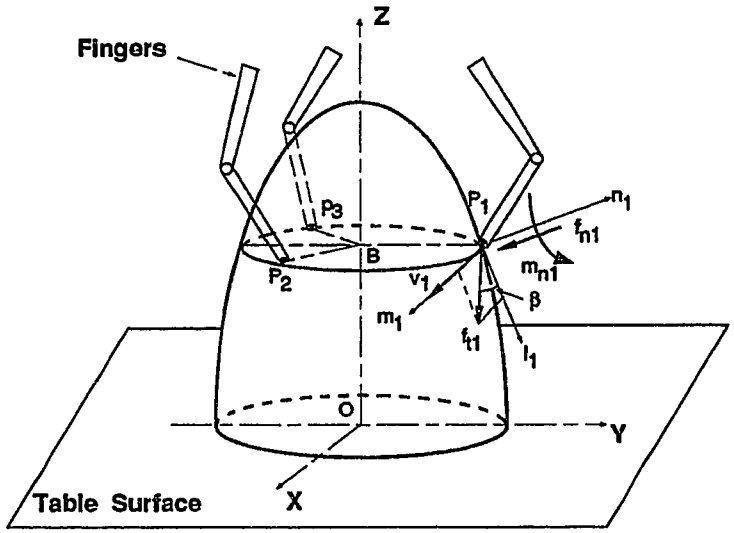

Figure 3.1: Hemi-ellipsoid grasped by three soft robotic fingertips

2. The grasped object is rigid. Its surface is smooth and continuous, *i.e.*, the equation of the object surface has the continuous second derivative.

3. The motion of object is slow enough that the static force and moment equilibrium equations can be applied at contact points.

4. Three dimension friction limit surface is assumed.

The object that we chose to explain the scheme of dextrous sliding analysis in three-dimensional case is a hemi-ellipsoid, as shown in Figure 3.1, where, P_1, P_2, and P_3 are three symmetric contact centroids between fingertips and the surface of ellipsoid. $O(XYZ)$ and $P_i(l_i m_i n_i)$ are the coordinate frames attached to the center of the ellipsoid and contact points, respectively. The surface of the grasped ellipsoid can be described, with respect to the XYZ axes, by the following equation

$$\frac{x^2}{a^2} + \frac{y^2}{b^2} + \frac{z^2}{c^2} = 1 \tag{3.1}$$

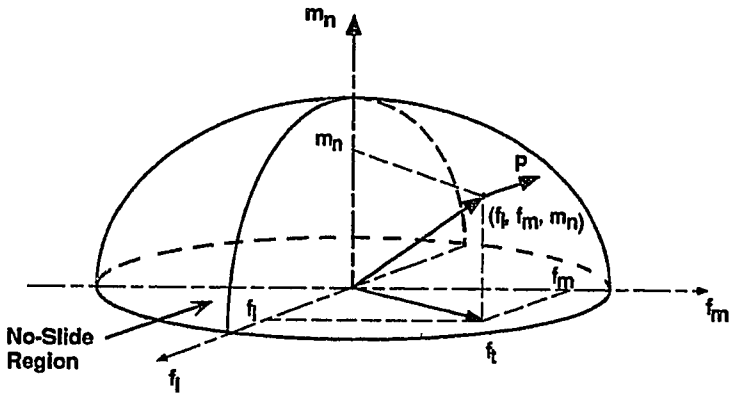

Figure 3.2: Friction limit surface in force/moment three-dimensional space

The trajectory planning problem in three-dimensional field is: "If we specify the motion of robotic fingertips, *i.e.*, the orentation and magnitude of the fingertips velocities at contacts, what will be the friction force (f_i) and moment (m_i) of the fingertips in order to result in a symmetric quasistatic sliding motion between fingertips and the surface of hemi-ellipsoid? Also, what will be the rotational motion of the object (ω), the sliding velocity (v_{si}), and the trajectories of the fingertips?"

3.2 Friction Limit Surface in 3D Space

When grasping an object, friction model always establishes the constraints to the force and moment that can be applied to the object. Therefore, all properties of friction limit surface in two-dimensional field can be used in three-dimensional field. Refer to Figure 3.2, f_l, f_m, and m_n are the friction force along the local axes l, m in the tangential plane and the friction moment normal to the surface of the grasped object at contact P_i, respectively. The surface of ellipsoid formed by these three components

is a criterion for quasistatic sliding motion in three-dimensional force/moment space, *i.e.*,

$$f_t^2 + \frac{m_n^2}{\lambda^2} = (\mu \cdot f_n)^2 \tag{3.2}$$

where, $f_t = \sqrt{f_l^2 + f_m^2}$, and $\lambda = \frac{m_{n,max}}{\mu \cdot f_n}$.

Similar to the 2D friction limit surface, an unit normal vector $\mathbf{P}$ to the friction limit surface represents the ratio of sliding velocity versus the rotational sliding velocity in tangential plane at each contact point P_i. If the friction force and moment are located inside the surface of friction limit surface, there is no sliding motion between the fingertips and the surface of object. Refer to Figure 3.2, we call it *no-sliding region*. When we increase the friction force and moment to the surface of the 3D friction limit surface, sliding motion will be initialed without acceleration. Beyond the 3D friction limit surface, acceleration of sliding will occur. The properties of the 3D friction limit surface are the criterion of friction force and moment of the fingers.

3.3 Force and Moment Equilibrium

Suppose the object grasped by the soft fingers is moving up with a small linear constant velocity v_b (0.5 cm/s), as shown in Figure 3.1. While we grasp and rotate the object, the dextrous sliding motion exists between the fingertips and the surface of the object. In order to predict the sliding trajectories and the motion of the object, we have to apply the appropriate force and moment by the fingers.

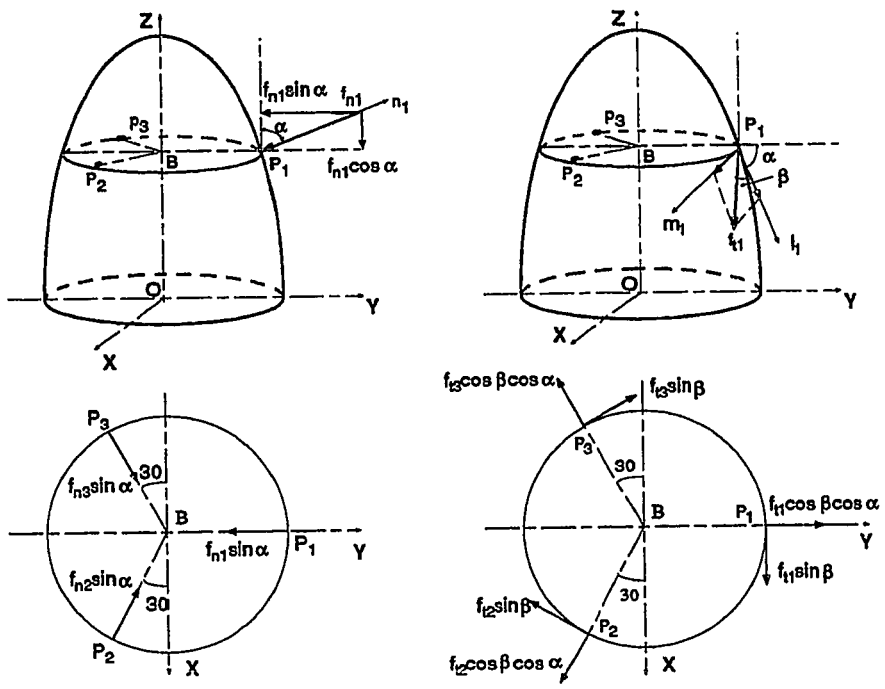

Figure 3.3: Grasp and friction force at contact points

The first constraint about force and moment is the 3D friction limit surface (refer to Figure 3.2), and the second constraint is the force/moment equilibrium equations. According to the object coordinate system $O(XYZ)$, the force/moment equilibrium equations can be expressed as follows

$$\begin{cases} \mathbf{F} = \sum_{i=1}^{3} \mathbf{f}_i + \mathbf{F}_b = 0 \\ \mathbf{M} = \sum_{i=1}^{3} (\mathbf{r}_i \times \mathbf{f}_i + \mathbf{m}_{ni}) + \mathbf{M}_b = 0 \end{cases} \tag{3.3}$$

where, $\mathbf{f}_i$ and $\mathbf{m}_{ni}$ are force and moment of fingertips, respectively.

At each contact point, in terms of local coordinate system $P_i(l_i m_i n_i)$, there are normal force $\mathbf{f}_{ni}$, friction force $\mathbf{f}_{ti}$, and moment $\mathbf{m}_{ni}$, as shown in Figure 3.1. For convenience, we express these vectors in the object coordinate system $O(XYZ)$, *i.e.*,

Normal force $\mathbf{f}_n$ shown in Figure 3.3 will be:

$$\begin{cases} \mathbf{f}_{n1} = 0 \cdot \mathbf{i} - f_{n1} \cdot \sin\alpha \cdot \mathbf{j} - f_{n1} \cdot \cos\alpha \cdot \mathbf{k} \\ \mathbf{f}_{n2} = -f_{n2} \cdot \sin\alpha \cdot \sin 30^\circ \cdot \mathbf{i} + f_{n2} \cdot \sin\alpha \cdot \sin 30^\circ \cdot \mathbf{j} - f_{n2} \cdot \cos\alpha \cdot \mathbf{k} \\ \mathbf{f}_{n3} = f_{n3} \cdot \sin\alpha \cdot \cos 30^\circ \cdot \mathbf{i} + f_{n3} \cdot \sin\alpha \cdot \sin 30^\circ \cdot \mathbf{j} - f_{n3} \cdot \cos\alpha \cdot \mathbf{k} \end{cases} \tag{3.4}$$

Friction force $\mathbf{f}_t$ shown in Figure 3.3 will be:

$$\begin{cases} \mathbf{f}_{t1} = f_{t1} \cdot \sin\beta \cdot \mathbf{i} + f_{t1} \cdot \cos\beta \cdot \cos\alpha \cdot \mathbf{j} - f_{t1} \cdot \cos\beta \cdot \sin\alpha \cdot \mathbf{k} \\ \mathbf{f}_{t2} = f_{t2}(c\beta c30^\circ - s\beta s30^\circ) \cdot \mathbf{i} - f_{t2}(c\beta c\alpha s30^\circ + s\beta c30^\circ) \cdot \mathbf{j} - f_{t2} c\beta s\alpha \cdot \mathbf{k} \\ \mathbf{f}_{t3} = -f_{t3}(c\beta c\alpha c30^\circ + s\beta s30^\circ) \cdot \mathbf{i} + f_{t3}(-c\beta c\alpha s30^\circ + s\beta c30^\circ) \cdot \mathbf{j} - f_{t3} c\beta s\alpha \cdot \mathbf{k} \end{cases} \tag{3.5}$$

where, $\mathbf{i}$, $\mathbf{j}$, and $\mathbf{k}$ are unit vectors along X, Y, and Z coordinates, and the prefix "s" and "c" to an angle denotes sine and cosine function, respectively.

If we apply the moment equilibrium Equation (3.3) with respect to the center point B, the fingertips position can be expressed as

$$\mathbf{r}_1 = \begin{bmatrix} 0 \\ r \\ 0 \end{bmatrix}, \mathbf{r}_2 = \begin{bmatrix} r \cdot \cos 30^\circ \\ -r \cdot \sin 30^\circ \\ 0 \end{bmatrix}, \mathbf{r}_3 = \begin{bmatrix} -r \cdot \cos 30^\circ \\ -r \cdot \sin 30^\circ \\ 0 \end{bmatrix} \tag{3.6}$$

And friction moments are

$$\begin{cases} \mathbf{m}_{n1} = 0 \cdot \mathbf{i} - m_{n1} \cdot sin\alpha \cdot \mathbf{j} - m_{n1} \cdot cos\alpha \cdot \mathbf{k} \\ \mathbf{m}_{n2} = -m_{n2} \cdot sin\alpha \cdot cos30^\circ \cdot \mathbf{i} + m_{n2} \cdot sin\alpha \cdot sin30^\circ \cdot \mathbf{j} - m_{n2} \cdot cos\alpha \cdot \mathbf{k} \\ \mathbf{m}_{n3} = m_{n3} \cdot sin\alpha \cdot cos30^\circ \cdot \mathbf{i} + m_{n3} \cdot sin\alpha \cdot sin30^\circ \cdot \mathbf{j} - m_{n3} \cdot cos\alpha \cdot \mathbf{k} \end{cases} \tag{3.7}$$

Since $\mathbf{f}_i = \mathbf{f}_{ni} + \mathbf{f}_{ti}$, we can substitute equation (3.4), (3.5) and (3.6) into equation

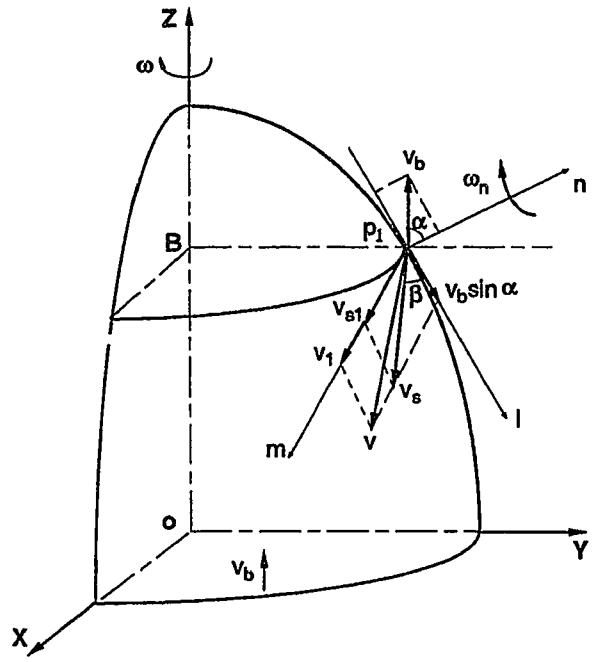

Figure 3.4: Velocities of the fingertips at contact

(3.3). Solving for the magnitude of $\mathbf{f}_n$, $\mathbf{f}_t$, and $\mathbf{m_n}$, we obtain,

$$\begin{cases} m_{n1} = m_{n2} = m_{n3} = m_n \\ f_{n1} = f_{n2} = f_{n3} = f_n \\ f_{t1} = f_{t2} = f_{t3} = f_t \end{cases} \tag{3.8}$$

$$\begin{cases} 3f_t \cdot \cos\beta \cdot \sin\alpha + 3f_n \cdot \cos\alpha = F_b \\ 3f_t \cdot \sin\beta \cdot r + 3m_n \cdot \cos\alpha = M_b \end{cases} \tag{3.9}$$

The expression of external moment (M_b) is shown in Appendix B.

3.4 Kinematics of Dexterous Sliding Motion

During sliding manipulation, in order for the fingertips to remain in contact with the surface of the ellipsoid, the velocity compatibility equations at each contact point need to be met. As shown in Figure 3.4, v_1 (0.5 cm/s) represents the fingertip absolute velocity and is always kept in local m axis. Sliding motion of the fingertips can be separated as linear and rotational components in local coordinates $P_i(l_i m_i n_i)$, *i.e.*,

$$\mathbf{v}_{slip} = \begin{bmatrix} v_s \cdot \cos\beta \\ v_s \cdot \sin\beta \\ \omega_n \end{bmatrix} \tag{3.10}$$

where the magnitudes of the linear sliding velocity and rotational sliding velocity is given by [Kao 1992]

$$\frac{v_s}{\omega_n} = \lambda^2 \cdot \frac{f_t}{m_n} \tag{3.11}$$

Since the object moves up with a constant linear velocity v_b, we can derive the velocity compatibility equations in local coordinates as

$$\begin{cases} v_1 = v_s \cdot \sin\beta + \omega_n \cdot r \cdot \cos\alpha \\ v_b \cdot \sin\alpha = v_s \cdot \cos\beta \end{cases} \tag{3.12}$$

Combining equation (3.9), (3.11), and (3.12), we obtain the friction force and moment as a function of sliding angle β, *i.e.*,

$$\begin{cases} f_t = \frac{r \cdot \sin 2\alpha}{\sin\alpha \cdot (r^2 - \lambda^2) \cdot \sin\beta + (\lambda^2 - r \cdot \sin^2\alpha) \cdot \cos\beta} \\ m_n = \frac{2\lambda^2 \cdot (\cos\beta - \sin\alpha \cdot \sin\beta)}{\sin\alpha \cdot (r^2 - \lambda^2) \cdot \sin\beta + (\lambda^2 - r \cdot \sin^2\alpha) \cdot \cos\beta} \end{cases} \tag{3.13}$$

For convinence, we define $A = \sin\alpha \cdot (r^2 - \lambda^2)$ and $B = \lambda^2 - r \cdot \sin^2\alpha$, then, equation (3.13) becomes

$$\begin{cases} f_t = \frac{r \cdot \sin 2\alpha}{A \cdot \sin\beta + B \cdot \cos\beta} \\ m_n = \frac{2\lambda^2 \cdot (\cos\beta - \sin\alpha \cdot \sin\beta)}{A \cdot \sin\beta + B \cdot \cos\beta} \end{cases} \tag{3.14}$$

Substituting the intermediate solution of friction force and moment *i.e.*, equation (3.14), into 3D friction limit surface, equation (3.2), yields,

$$\frac{r^2 \cdot \sin^2 2\alpha}{4(A\sin\beta + B\cos\beta)^2} + \frac{\lambda^2(\cos\beta - \sin\alpha \cdot \sin\beta)^2}{(A\sin\beta + B\cos\beta)^2} = 1 \tag{3.15}$$

Solving for sliding angle β from equation (3.15), we can find the trajectory of the robotic fingertips and the rotational velocity of the object, simulation of the above results will be presented in section 4.3. The simulation program is in Appendix C.

Chapter 4

Simulation Results and Discussion

4.1 Overview

The simulation results will be addressed in Section 4.2 and 4.3 in terms of 2D and 3D field. 2D simulation program is based on the business card example. The program simulates the instantaneous motion of the object, equation (2.9), as well as the trajectories of the fingertips, equation (2.11). Results and discussion will be followed. The programs and results are shown in Appendix C.

Section 4.3 shows the simulation results of the fingertips trajectories in 3D space, equation (3.15), and the motion of object, equation (3.11). Also, we discuss the effects of the friction moment on the rotational motion of the object.

4.2 2D Simulation Results and Discussion

The trajectory of the sliding fingertips with respect to the XY coordinates is shown in Figure 2.5. One can verify this trajectory by sliding two thumbs on a business card, while maintaining the forces of thumbs horizontal and equal in magnitude. It can be observed that the card will rotate and fingertips will be sliding on the card until both thumbs are aligned with each other – at which point the card stops though the thumbs will keep on moving with no net rigid-body motion, *i.e.*, the card does not move. When the rotation angle q is small, the trajectory agrees with the results that we have already known from the previous theory and experiments. As the rotation angle (q) becomes larger, the angular velocity of the card (ω) gradually decreases until it becomes zero. Note that the independent parameter τ* is not explicitly expressed in Figure 2.5. A plot of ω with respect to simulation steps is shown in Figure 4.1. It is also observed during the experiments of [Kao and Cutkosky 1993] that as the fingers move to the end of the travel (about $q = 20°$), the trajectory of the fingers starts to deviate from the circular profile for instantaneous motion. Figure 2.5 indicates this phenomena clearly.

At the starting point of Figure 4.1 when $\tau = 0$, the same external force produces more rotations on the grasped object; whereas, at the end, such external force causes very little RB motion. Finally, the velocity of the card asymptotically approaches zero in the simulation. This result shows an important observation that there are

*The parameter τ is equivalent to the time in dynamic motion simulation.

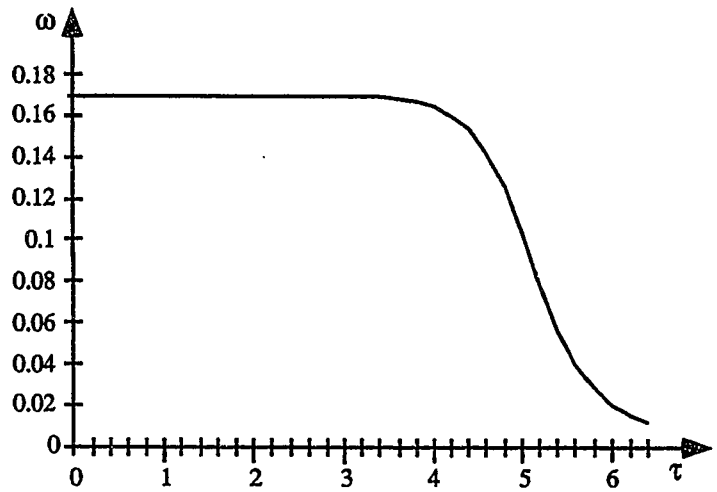

Figure 4.1: Angular velocity of the card, ω, vs. the independent parameter, τ. As τ increases, ω decreases and approaches zero asymptotically.

orientations for which external forces can produce more effective RB motions. We call such orientations the *advantageous orientations.* With the same external forces, we may want to be at such advantageous orientations if our objective is to move the grasped object more effectively. There are times, however, that we want to cause the least RB motions – in which case, we will arrange the orientation in such a way that it produces more NRB motions. This result can be applied in motion planning to find the desired orientations of the external force/motion to produce the required motions of the grasped object.

Figure 4.2 shows a typical history of the RB and NRB motions throughout the sliding manipulation. We have seen that as q increases, the angular velocity of the card, ω, decreases. This can be shown clearly in the figure where the RB component diminishes and the NRB component increases as the times elapsed. Finally when $q = 90°$, $\mathbf{v}_1$ and $\mathbf{v}_2$ align with each other and the velocity of the card changes to

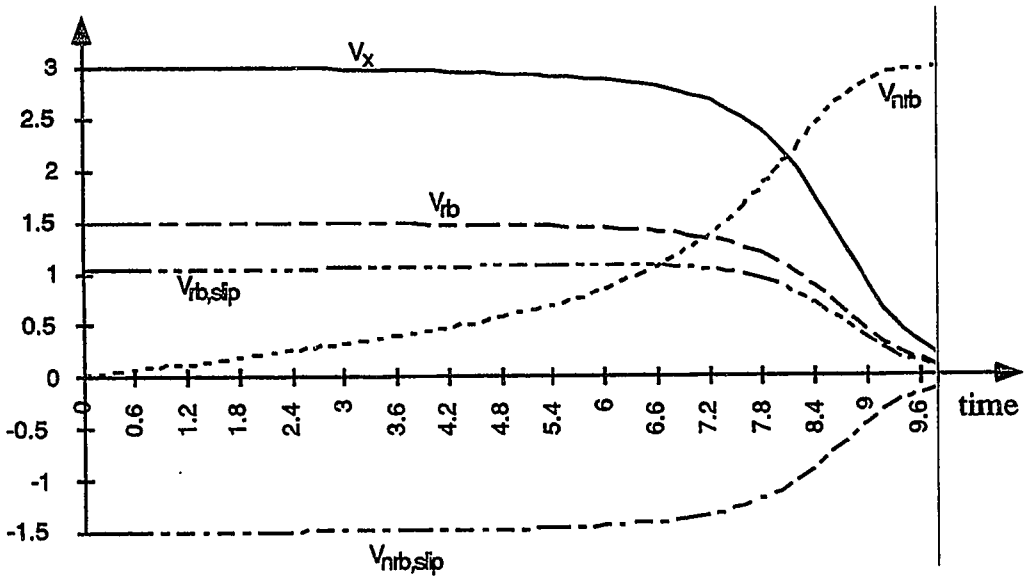

Figure 4.2: Velocities of fingertips showing the RB and NRB components for the sliding manipulation. The manipulation starts with large effective RB components and ends with only NRB components when the card stops moving.

NRB motion only. Studying the RB/NRB plot, therefore, can provide us with useful information about the motion of the grasped object.

It is also noted that when we change the characteristic length (r) of the weighting matrix ($\mathbf{W}$), we scale the RB and NRB operation spaces and hence alter the magnitudes of RB and NRB velocities in that particular operation space. Nonetheless, the solution for the angular velocity of the grasped object, ω, remains unchanged.

4.3 3D Simulation Results and Discussion

Trajectory planning task with multi-soft fingers in 3D field is carried out under a motion control scheme as shown in Figure 3.1, where the grasped object is moved with

a linear constant velocity. We proposed this particular problem in order to illustrate the steps to implement a dexterous sliding analysis in 3D field. Our solution is based upon the contact configuration and the 3D friction limit surface. The simulation result of the fingertip trajectory is shown in Table 4.1.

As we can see from Table 4.1, 3D trajectory generated by motion control scheme at contact is predictable under some assumptions. For a desired trajectory of the fingertips, we can find the dextrous sliding motion of the fingertips first, then combine it with the motion of the object to obtain the desired trajectory of the fingertips. Throughout the theoretical analysis and simulation program, we can adjust the ratio of friction force and moment through the 3D friction limit surface, fingertips absolute velocity to get the different results.

RB motion is still the main factor to affect the rotation of the grasped object. Refer to Figure 3.1, if we keep the fingers velocities (v_i) in local l_i axis, there is no friction moment at contacts. Fingertips velocities are pure NRB and no RB motion exists. So there is no rotational motion of the object. When we change the orientation and magnitude of the fingertips velocities (v_i), different rotio of RB and NRB can be created. Therefore, desired trajectories of the fingertips and the rotational velocity of the object can be obtained through our simulation programs.

$Time(s)$	X	Y	Z	$Time(s)$	X	Y	Z
0	0	1.8	4	4	1.290	2.256	2.497
0.5	0.172	1.908	3.848	4.5	1.427	2.259	2.274
1	0.344	2.000	3.683	5	1.556	2.252	2.046
1.5	0.513	2.075	3.508	5.5	1.678	2.236	1.812
2	0.679	2.136	3.323	6	1.792	2.213	1.575
2.5	0.840	2.184	3.128	6.5	1.897	2.182	1.335
3	0.996	2.220	2.925	7	1.994	2.144	1.092
3.5	1.147	2.24	2.715	7.5	2.082	2.099	0.846

Table 4.1 Data of the fingertip trajectory with respect to $P(XYZ)$ coordinate system.

The rotational velocity of the object depends on the friction moment applied by the multi-soft-fingertip at contacts. The magnitude of the rotational velocity (ω) is directly related to the ratio of the friction force and moment at contacts, as seen in equation (3.11). At the end of manipulation, the anglular velocity (ω) is near a constant because the ratio of fingertips friction force and moment tends to be a constant. As we noticed from Figure 4.3, this relationship can be obtained from our simulation results.

As we knew from previous research, fingertips sliding velocities will always be in the same direction as the friction force during manipulation. Grasping a moving elliptical surface object with three fingertips as described in Chapter 3 and rotate your

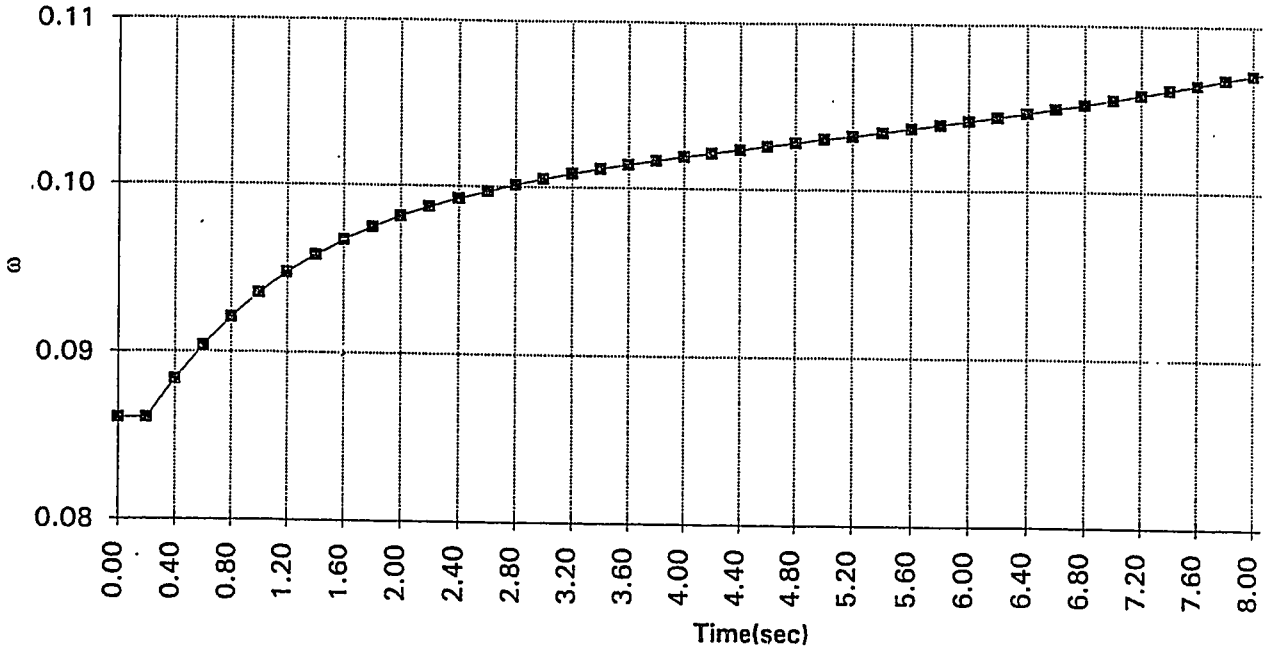

Figure 4.3: Rotational velocity of the object with respect to the object coordinate system $P(XYZ)$

fingertip to start a sliding motion, one can observe the direction of your fingertips sliding motion. Sliding motion will begin with a large sliding angle β and end up with a constant sliding angle (smaller). Figure 4.4 is the simulation result of the sliding angle β in the 3D example. The fingertips sliding angle β is graduately reduced from 43° to 20°. The sliding angle β approaches a constant asymptotically as a function of the time.

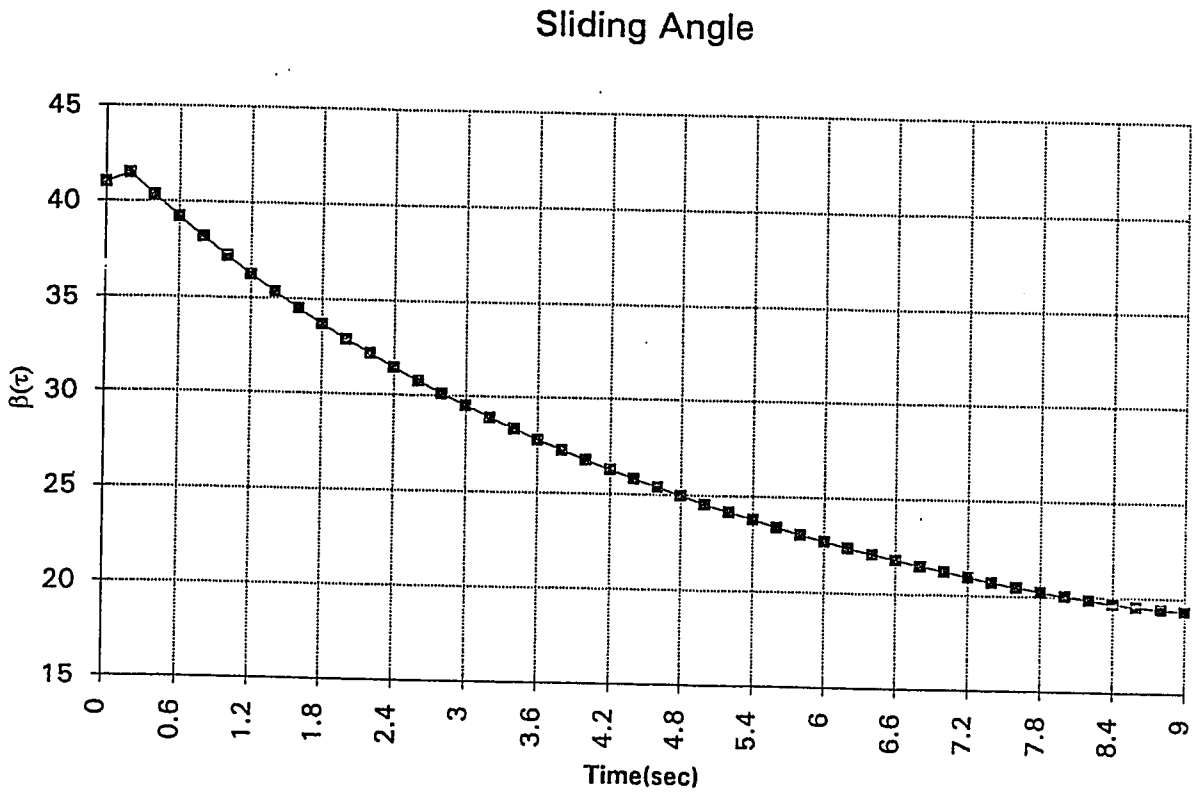

Figure 4.4: Fingertip sliding angle with respect to the local coordinate system $P_i(l_i m_i n_i)$

Chapter 5

Conclusion and Future Work

5.1 Conclusions

We conclude from the study of dextrous manipulation that,

1. The basic requirements in dextrous sliding analysis, (i) friction limit theorey establishs the first constaint for the grasped force and moment; (ii) static force and moment equilibrium can be applied to the slow motion manipulation, *i.e.*, the motion of the fingertips as well as the object are slow; (iii) velocity compatibility has to be satisfied at contacts.

2. The dextrous sliding analysis with RB/NRB can be applied to trajectory planning over finite range of motions. The relative magnitudes of RB/NRB motion is an index for manipulation task. In addition, by careful planning of the advantageous orientation of the external forces/moments and motions, we can

produce more effective RB motions of the grasped object. On the contrary, one can also plan forces such that minimal RB motions of the object is achieved.

3. The extension of dextrous sliding analysis of 3D trajectory planning problems lead us to define and analyze a general 3D example. The result shows that once we have the grasped configuration, we can implement the dextrous sliding analysis to our planning tasks. Therefore, the dextrous sliding analysis can be a general scheme for trajectory and motion planning.

5.2 Future Work

Since the 2D program can simulate the motion of the object and fingers simutaneously, we need to set up the experiment to compare with the simulation results. In 3D field, we will consider the unsymmetrical contacts in order to explore general 3D dextrous sliding analysis. The method of RB/NRB decomposition and limit surface needs to be extended to 3D dynamic manipulation.

Appendix A

Derivation of Equations in Chapter 2

A.1 Jacobians of Two Fingertips

$$ {}^{P}_{B}\mathbf{J}_1 = \begin{bmatrix} \cos(q) & -\sin(q) & -r \\ \sin(q) & \cos(q) & 0 \\ 0 & 0 & 1 \end{bmatrix} \tag{A.1} $$

$$ {}^{P}_{B}\mathbf{J}_2 = \begin{bmatrix} \cos(q) & -\sin(q) & r \\ \sin(q) & \cos(q) & 0 \\ 0 & 0 & 1 \end{bmatrix} \tag{A.2} $$

A.2 The Weighting Matrices

The weighting matrices are chosen with r as the characteristic length, that is,

$$\mathbf{W}_1 = \mathbf{W}_2 = \begin{bmatrix} 1 & 0 & 0 \\ 0 & 1 & 0 \\ 0 & 0 & r^2 \end{bmatrix} \tag{A.3}$$

A.3 RB/NRB Components of the Fingertips

The RB and NRB components of the manipulation are listed as functions of the angles β, q, and the velocities of the fingertips.

$$\mathbf{v}_{rb} = \begin{bmatrix} \frac{1}{2} \cdot v \cdot \cos(\beta) \\ 0 \\ -\frac{1}{2r} \cdot v \cdot \cos(\beta) \end{bmatrix} \tag{A.4}$$

$$\mathbf{v}_{nrb} = \begin{bmatrix} \frac{1}{2} \cdot v \cdot \cos(\beta) \\ v \cdot \sin(\beta) \\ \frac{1}{2r} \cdot v \cdot \cos(\beta) \end{bmatrix} \tag{A.5}$$

$$\mathbf{v}_{rb,slip} = \begin{bmatrix} -\frac{v \cdot \cos(\beta)}{\sin(q)} + \frac{1}{2} \cdot v \cdot \cos(\beta) \\ 0 \\ \frac{1}{2} \cdot v \cdot \cos(\beta) \end{bmatrix} \tag{A.6}$$

$$\mathbf{v}_{nrb,slip} = \begin{bmatrix} -\frac{1}{2} \cdot v \cdot \cos(\beta) \\ -v \cdot \sin(\beta) \\ -\frac{1}{2r} \cdot v \cdot \cos(\beta) \end{bmatrix} \tag{A.7}$$

Appendix B

Derivation of Equations in Chapter 3

B.1 Solving the Sliding Angle β

Form equation (3.15), we can form the following equation for β

$$C \cdot \tan^2 \beta + D \cdot \tan \beta + E = 0 \tag{B.1}$$

where the intermediate variables C, D, and E are defined as

$$\begin{cases} C = r^2 \cdot \sin^2 2\alpha + 4\lambda^2 \cdot sin^2\alpha - 4A^2 \\ D = -8(A \cdot B + \lambda^2 \sin \alpha) \\ E = r^2 \cdot sin^2 2\alpha + 4\lambda^2 - 4B^2 \end{cases} \tag{B.2}$$

Since A, B, C, D, and E are all depend on the contact position **r** and geometry parameters, we can solve the sliding angle (β) from equation (B.1).

B.2 Geometry Parameters

According to equation 3.1, we choose the geometry parametry as $a = b = 3cm$ and $c = 5cm$. Therefore, equation 3.1 becomes

$$\frac{x^2}{9} + \frac{y^2}{9} + \frac{z^2}{25} = 1 \tag{B.3}$$

In YZ plane, $\tan\theta = \frac{9}{25} \cdot \frac{z}{y}$, *i.e.*, $\theta = \arctan(\frac{9z}{25y})$. So, $\alpha = 90 - \theta$.

B.3 The expression of External Moment M_b

Assume the contact area between the object and table surface has the constant force distrubution. Then, the external moment M_b can be derived as

$$M_b = \int_0^R \frac{2\pi \cdot r \cdot dr}{\pi \cdot R^2} F_b \cdot \mu \cdot r = \frac{2}{3} \cdot \mu \cdot R \cdot F_b = F_b \tag{B.4}$$

Appendix C

Simulation Programs

C.1 Manipulating a Card with Two Sliding Soft Fingertips

```
#include<conio.h>

#include<graph.h>

#include<stdlib.h>

#include<malloc.h>

#include<string.h>

#include<stdio.h>

#include<math.h>

#define  pi  3.14159

void  freeze_screen(void);
```

```
void  ini(void);

main()

{

float r, fn, ft, mu, m_max, mn, v, lambda, w, z, s, delt_q1;

float cot_psi, vslip, q, t, x, y, w0, vslip_x0, scale;

char text1[64]

/* Knowns */

t=0; q=0; x=0; y=0.015; fn=1.0; mu=0.38;

m_maw=0.00247; v=0.003; z=0; scale=6000;

ini();

lambda=m_max/(mu*fn);

ft=mu*fn*lambda/(sqrt(lambda*lambda+r*r));

mn=r*ft;

cot_psi=lambda*ft/mn;

w0=v/(r+lambda*cot_psi);

vslip_x0=w0*lambda*cot_psi;

/* Setup  initial  position  of  the  card */

sprintf(text1,''The trajectory of two soft fingertips sliding on a card'');

_settextposition(200,12);

_outtext(text1);

sprintf(text1,''Y'');

_settextposition(5,39);
```

```
_outtext(text1);

sprintf(text1,''X'');

settextposition(16,68);

_outtext(text1);

sprintf(text1,''COR'');

_settextposition(16,37);

_outtext(text1);

sprintf(text1,''w0 =%f(rad) vslip_x0 = %f(m/s)'',w0, vslip_x0);

_settextposition(2,20);

_outtext(text1);

_moveto(-190,0);

_lineto(195,0);

_moveto(0,170);

_lineto(0,-170);

_rectangle(_GBORDER,-.018*scale,-.024*scale,.018*scale,.024*scale);

_rectangle(_GBORDER,-310,-235,310,208);

_setcolor(10);

_setpixel(20,-y*scale);

_setpixel(-20,y*scale);

_setcolor(14);

_arc(-90,-90,90,90,120,0,0,-120);

_arc(-90,-90,90,90,-120,0,0,120);
```

```
while(y > 0.0001);
{
t+=1;
ft=mu*fn*lambda/(sqrt(pow(lambda,2)+r*r*cos(q)*cos(q)));
mn=ft*r*cos(q);
cot_psi=lambda*ft/mn;
w=v*cos(q)/(r+lambda*cot_psi*cos(q));
delt_q1=1*w;
z+=delt_q1;
s=180*z/pi;
vslip=w*lambda*cot_psi;
y=r*cos(q+1*w);
x=r*sin(q+1*w)+vslip*1;
for(j=1; j < 300000; j++);
{}
sprintf(text1,''t= %f s w= %f r/s q= %f d x= %m y= %m'', t, w, q, x, y);
_settextposition(3,8);
_outtext(text1);
_setcolor(11);
_setpixel(x*scale,-y*scale);
_setpixel(-x*scale,y*scale);
q=pi/2.0-atan2(y,x);
```

```
r=sqrt(x*x+y*y);
_setcolor(4);
_moveto(.03*cos(-z+53.13*pi/180)*scale,-.03*sin(-z+53.13*pi/180)*scale);
_lineto(.03*cos(z+53.13*pi/180)*scale,.03*sin(z+53.13*pi/180)*scale);
_lineto(-.03*cos(-z+53.13*pi/180)*scale,.03*sin(-z+53.13*pi/180)*scale);
_lineto(-.03*cos(z+53.13*pi/180)*scale,-.03*sin(z+53.13*pi/180)*scale);
_lineto(.03*cos(-z+53.13*pi/180)*scale,-.03*sin(-z+53.13*pi/180)*scale);
}
_moveto(190*sin(z),-190*cos(z));
_lineto(-190*sin(z),190*sin(z));
_moveto(190*cos(z),1908sin(z));
_lineto(-190*cos(z),-190*sin(z));
_arc(-20,-20,20,20,20*sin(z),-20*cos(z),0,-20);
sprintf(text1,''q'');
_settextposition(14,43);
_outtext(text1);
freeze_screen();
}
void  ini(void)
{
struct  videoconfig  vc;
_setvideomode(_VRES16COLOR);
```

```
_getvideoconfig(&vc);

_setlogorg(320,240);

_clearscreen(_GCLEARSCREEN);

}

void  freeze_screen(void)

{

getch();

_setvideomode(_DEFAULTMODE);

}
```

C.2 Manipulating a Hemi-ellipsoid Using Three Soft Fingers

```
#include<conio.h >

#include<graph.h >

#include<stdlib.h>

#include<malloc.h>

#include<string.h>

#include<stdio.h >

#include<math.h  >

#define pi 3.14159

void freeze_screen(void);

void  ini(void);

main()

{

FILE  *fp_in;

float  x,y,z,r,vb,v1,fn,ft,mn,vs,wn,A,B,C,D,E,F,lambda;

float  thetar,theta,betar,beta,alphar,alpha,psir,psi;

float  ds1,ds2,dz,t,dt,pp,i;

char  text1[64]

/* Knowns */

x=0; y=1.8; r=1.8; vb=0.5; v1=0.5; fn=1; lambda=0.35;
```

```
t=0; dt=0.5; psir=0;

ini();

fp_in=fopen(''traj3.dat'',''w'');

sprintf(text1,''\t 3-D Simulation Data File \t Done By Ying Xue \n'');

fputs(text1,fp_in);

sprintf(text1,''-------------------------------------------\n'');

fputs(text1,fp_in);

sprintf(text1,'' t       x y z \n'');

fputs(text1,fp_in);

sprintf(text1,''-------------------------------------------\n'');

fputs(text1,fp_in);

sprinf(text1,'' %f %f %f %f  \n'',t,x,y,z);

fputs(text1,fp_in);

while(z > 1)

{

/* Find alpha */

y=r;

thetar=atan(9*z/(25*y));

theta=thetar*180/pi;

alphar=pi/2-thetar;

alpha=alphar*180/pi;

/* Find beta */
```

```
A=(r*r-pow(lambda,2))*sin(alphar);

B=pow(lambda,2)-r*pow(sin(alphar),2);

C=pow(r*sin(2*alphar),2)+4*pow(lambda*sin(alphar),2)-4*A*A;

D=8*(A*B+sin(alphar)*pow(lambda,2));

E=pow(r*sin(2*alphar),2)+4*pow(lambda,2)-4*B*B;

betar=atan((-D-sqrt(D*D-4*C*E))/(2*C));

beta=betar*180/pi;

/* Find friction force ft, moment mn and motion */

F=A*sin(betar)+B*cos(betar);

ft=r*sin(2*alphar)/F;

mn=2*pow(lambda,2)*(cos(betar)-sin(alphar)*sin(betar))/F

vs=sin(alphar)/(2*cos(betar));

wn=mn*sin(alphar)/(2*pow(lambda,2)*ft*cos(betar));

/* Print results */

sprintf(text1,''alpha= % f,beta= % f'',alpha,beta);

_settextposition(2,1);

_outtext(text1);

sprintf(text1,''ft=%f,mn=%f,vs=%f,wn=%f'',ft,mn,vs,wn);

_settextposition(4,1);

_outtext(text1);

/* Find the trajectory of the sliding fingertip */

t=t+dt;
```

```
ds1=0.5*sin(alphar)*dt;

dz=ds1*sin(alphar);

z=z-dz;

r=3*sqrt(1-z*z/25);

ds2=vs*sin(betar)*dt;

pp=ds2/r;

psir=psir+pp;

psi=psir*180/pi;

x=r*sin(psir);

y=r*cos(psir);

sprintf(text1,'' %f  %f  %f  %f\n'',t,x,y,z);

fputs(text1,fp_in);

}

fclose(fp_in);

freeze_screen();

}

void ini(void)

{

struct videoconfig  vc;

_setvideomode(_VRES16COLOR);

_getvideoconfig(&vc);

_setlogorg(50,240);
```

```
_clearscreen(_GCLEARSCREEN);

}

voil freeze_screen(void)

{

getch();

_setvideomode(_DEFAULTMODE);

}
```

Bibliography

[1] Chong, N. Y.; Choi, D.; and Suh, I. H. 1993. A finite motion planning strategy for multifingered robotic hands considering sliding and rolling contacts. In *IEEE International Conference on Robotics and Automation.* Pages 180–187.

[2] Goyal, Suresh; Ruina, Andy; and Papadopoulos, Jim 1991. Planar sliding with dry friction: Part 1. limit surface and moment function. *Wear* Pages 307–330.

[3] Kao, I. and Cutkosky, M. R. 1989. Dextrous manipulation with compliance and sliding. In *The 5th International Symposium on Robotics Research*, Tokyo, Japan. MIT Press.

[4] Kao, I. and Cutkosky, M. R. 1992. Dextrous manipulation with compliance and sliding. *International Journal of Robotics Research* 11(1):20–40.

[5] Kao, I. and Cutkosky, M. R. 1993. Comparison of theoretical and experimental force/motion trajectories for dextrous manipulation with sliding. *Int. Journal of Robotics Research.*

[6] Lee, S.-H. 1991. *Automatic Fixture Planning in Small Batch Manufacturing.* Ph.D. Dissertation, in preparation, Department of Mechanical Engineering, Stanford University.

[7] Mason, M. T. and Salisbury, J. K. 1985. *Robot Hands and the Mechanics of Manipulation.* The MIT Press.

[8] Mason, M. T. 1985. On the scope of quasi-static pushing. In *The Proceedings of Third International Symposium on Robotics Research.*

[9] Michelman, Paul and Allen, Peter 1993. Compliant manipulation with a dextrous robot hand. In *IEEE International Conference on Robotics and Automation.* Pages 711–716.

[10] Montana, David J. 1988. The kinematics of contact and grasp. *The International Journal of Robotics Research* 7(3):17–32.

[11] Peshkin, M. A. and Sanderson, A. C. 1988a. The motion of a pushed, sliding workpiece. *IEEE journal of Robotics and Automation* 4(6):569–598.

[12] Peshkin, M. A. and Sanderson, A. C. 1988b. Planning robotic manipulation strategies for workpieces that slides. *IEEE journal of Robotics and Automation* 4(5):524–531.

[13] Rus, Daniela 1992. Dextrous rotations of polyhedra. In *IEEE International Conference on Robotics and Automation.* Pages 2758–2763.

[14] Sarkar, Nilanjan; Yun, Xiaoping; and Kumar, Vijay 1993. Dynamic control of a 3-d rolling contacts in two-arm manipulation. In *The Proceedings of 1993 IEEE International Conference on Robotics and Automation*, Cambridge, MA. MIT Press. Pages 978–983.

[15] Trinkle, J. C. 1989. A quasi-static analysis of dexterous manipulation with sliding and rolling contacts. In *Proceedings of 1989 IEEE Conference on Robotics and*

Automation. Pages 788–793.

[16] Y. Xue and I. Kao 1994. *MAL Technical Report No. MAL-9303, SJSU.* Dextrous sliding manipulation using two soft fingertips. In *IEEE International Confence on Robotics and Automation.*

[17] Ian D. Walker, Robert A. Freeman, and Steven I. Marcus 1991. Analysis of Motion and Internal Loading of Objects Grasped by Multiple Cooperating Manipulators. In *The International Journal of Robotics Research, Vol. 10, No. 4, August 1991.* Pages 396-398

[18] David J. Montana 1992. Contact Stability for Two-Fingered Grasps. *IEEE Transactions on Robotics and Automation.* Vol. 8. No. 4, August 1992

[19] Tsuneo Yoshikawa and Kiyoshi Nagai 1991, Manipulation and Grasping Forces in Manipulation by Multifingered Robot Hands. *IEEE Transactions of Robotics and Automation* Vol. 7 No. 1, February 1991